

## Kinetics of Unfolding the Human Telomeric DNA Quadruplex Using a PNA Trap

Jeremy J. Green, Liming Ying, David Klenerman,\* and Shankar Balasubramanian\*

Contribution from the Department of Chemistry, University of Cambridge, Lensfield Road, Cambridge, CB2 1EW, U.K.

Received October 30, 2002; E-mail: sb10031@cam.ac.uk; dk10012@cam.ac.uk

**Abstract:** The kinetics of opening of the DNA quadruplex formed by the human telomeric repeat have been investigated using real-time fluorescence resonance energy transfer (FRET) measurements with a peptide nucleic acid (PNA) trap. It has been found that this opening is zero-order with respect to PNA, indicating that the initial step is a rate-limiting internal rearrangement of the quadruplex. A study of the temperature dependence of the rate of quadruplex opening was performed and the activation energy of the process estimated to be  $98 \pm 8$  kJ mol<sup>-1</sup>.

### Introduction

DNA sequences with multiple guanine stretches can form four-stranded inter- and intramolecular quadruplex structures that may be important for a number of biological processes and disease-related mechanisms.<sup>1,2</sup> In particular G-quadruplex DNA formed from telomeric sequence repeats may be important for telomere maintenance<sup>3,4</sup> and DNA replication<sup>5</sup> and is a potential target for novel anticancer drugs.<sup>6,7</sup> Quadruplexes arise due to the ability of guanines to hydrogen bond in a cyclic fashion to form tetrads (Chart 1a). These tetrads can stack with a helical twist to form quadruplex structures (Chart 1b). Such structures can be further stabilized by interactions between O6 of guanine with cations, particularly monovalent metal ions.

G-quadruplexes are highly polymorphic, and a large number of different structures have been observed.<sup>1,8</sup> For example a sequence containing a single run of guanine can form only a tetrameric quadruplex, while sequences with multiple G-tracts may, depending on the conditions, form hairpin dimers or intramolecular quadruplexes.

FRET is the distance-dependent transfer of energy from a donor fluorophore to an acceptor. It is useful for measuring distances on the 1–10 nm scale<sup>9,10</sup> and is a valuable tool for the structural analysis of biomolecules.<sup>11,12</sup> A quadruplex-forming oligonucleotide with a donor and acceptor attached to

**Chart 1.** (a) Tetrad Showing Hydrogen Bonds between Guanines and the Interaction with a Cation (shaded circle); (b) Schematic of a G-Quadruplex Showing Tetrads (translucent squares), the DNA Backbone (vertical lines), and Stabilizing Cations (shaded circles)

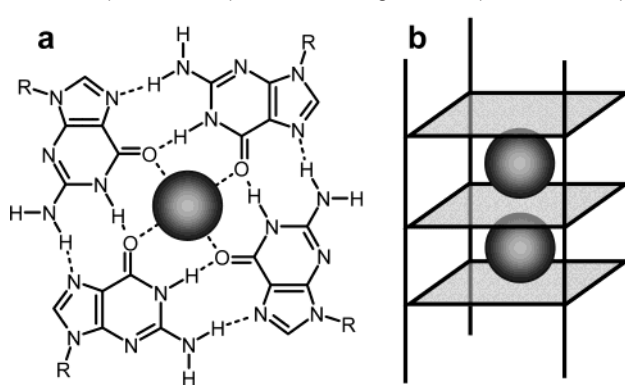
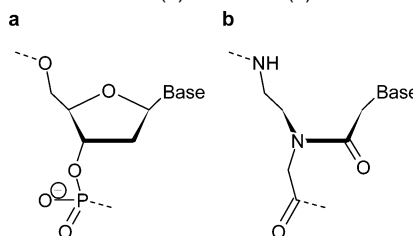


**Chart 2.** Structural Units of (a) DNA and (b) PNA



its termini shows a large change in FRET efficiency between the folded and unfolded conformers.<sup>13–15</sup>

Peptide nucleic acid (PNA) is a synthetic DNA analogue (Chart 2) with an uncharged 2-aminoethylglycine backbone.<sup>16</sup> It is able to hybridize to DNA and RNA with better sequence

- (1) Simonsson, T. *Biol. Chem.* **2001**, *382*, 621–628.
- (2) Arthanari, H.; Bolton, P. H. *Chem. Biol.* **2001**, *8*, 221–230.
- (3) Zahler, A. M.; Williamson, J. R.; Cech, T. R.; Prescott, D. M. *Nature* **1991**, *350*, 718–720.
- (4) Fletcher, T. M.; Sun, D.; Salazar, M.; Hurley, L. H. *Biochemistry* **1998**, *37*, 5536–5541.
- (5) Sen, D.; Gilbert, W. *Nature* **1988**, *334*, 364–366.
- (6) Kerwin, S. M. *Curr. Pharm. Des.* **2000**, *6*, 441–471.
- (7) Neidle, S.; Parkinson, G. *Nature Drug Discovery* **2002**, *1*, 383–393.
- (8) Williamson, J. R. *Annu. Rev. Biophys. Biomol. Struct.* **1994**, *23*, 703–730.
- (9) Latt, S. A.; Cheung, H. T.; Blout, E. R. *J. Am. Chem. Soc.* **1965**, *87*, 995–1003.
- (10) Stryer, L.; Haugland, R. P. *Proc. Natl. Acad. Sci. U.S.A.* **1967**, *58*, 719–726.
- (11) Lilley, D. M. J.; Wilson, T. J. *Curr. Opin. Chem. Biol.* **2000**, *4*, 507–517.
- (12) Selvin, P. R. *Nature Struct. Biol.* **2000**, *7*, 730–734.

- (13) Simonsson, T.; Sjöback, R. *J. Biol. Chem.* **1999**, *274*, 17379–17383.
- (14) Mergny, J.-L.; Maurizot, J.-C. *ChemBioChem* **2001**, *2*, 124–132.
- (15) Ueyama, H.; Takagi, M.; Takenaka, S. *J. Am. Chem. Soc.* **2002**, *124*, 14286–14287.
- (16) Nielsen, P. E.; Egholm, M.; Berg, R. H.; Buchardt, O. *Science* **1991**, *254*, 1497–1500.

specificity and thermodynamic stability than natural nucleic acids.<sup>17</sup> Recently a 7-mer PNA was shown to open the thrombin binding aptamer quadruplex, illustrating the ability to trap out complex structures with relatively short PNAs.<sup>18</sup>

Here we report studies of the kinetics of opening of the intramolecular quadruplex formed by a dual-labeled 21-mer oligonucleotide composed of 3.5 repeats of the human telomeric sequence, i.e., d[(GGGTTA)<sub>3</sub>GGG].<sup>19</sup> This sequence has been shown to form an intramolecular quadruplex in the presence of sodium and potassium ions.<sup>20</sup> We used FRET to monitor the unfolding of this structure using highly sensitive fluorescence measurements, with relatively small quantities of material.

## Experimental Section

**Materials.** The oligonucleotides 5'-d(GGGTTAGGGTTAGGGTTAGGG)-3' (**htelo**) and 5'-TMR-d(GGGTTAGGGTTAGGGTTAGGG)-Cy5-dT-3' (**htelo-fl**) (where Cy5 and tetramethylrhodamine (TMR) are fluorescent dyes) were obtained HPLC pure from Oswel (Southampton, UK) and used without further purification. These oligonucleotides were based on the minimal human telomere repeat sequence capable of forming an intramolecular quadruplex. The PNA oligomers H<sub>2</sub>N-TGTAAGGAAGTAG-Lys-CO<sub>2</sub>H (**nPNA**) and H<sub>2</sub>N-CTAACCCCTAACCC-Lys-CO<sub>2</sub>H (**cPNA**) were received HPLC pure as gifts from Dr. Yamuna Krishnan-Ghosh and Gérald Gavory and used without further purification. Tris·HCl (1 M, pH 7.4) was purchased from Sigma (Dorset, UK) and NaCl from Breckland (Norfolk, UK). Deionized water was obtained from an Elga Maxima or a MilliPore Milli-Q PLUS and used throughout.

The extinction coefficient at 260 nm ( $\epsilon_{260}$ ) of **htelo-fl** was calculated using a nearest-neighbor method<sup>21</sup> for the central 21-base sequence, adding the  $\epsilon_{260}$  values of TMR and Cy5 (31 980 and 10 000 M<sup>-1</sup> cm<sup>-1</sup>, respectively)<sup>22</sup> and the lone thymine at the 3' terminus. The  $\epsilon_{260}$  of **htelo** was provided by the manufacturer, and those of the PNAs were calculated by summing the  $\epsilon_{260}$  values of the individual PNA monomers (A, 13 700 M<sup>-1</sup> cm<sup>-1</sup>; C, 6600 M<sup>-1</sup> cm<sup>-1</sup>; T, 8600 M<sup>-1</sup> cm<sup>-1</sup>; G, 11 700 M<sup>-1</sup> cm<sup>-1</sup>).<sup>23</sup>

**Equipment.** UV measurements were performed using a Varian Cary 1E spectrophotometer equipped with a computer-controlled Peltier temperature controller. Fluorescence measurements were taken using an Aminco-Bowman Series 2 fluorimeter equipped with a water bath. Circular dichroism measurements were performed on a Jasco J-810 spectropolarimeter equipped with a computer-controlled Peltier temperature controller.

**Folding.** A solution of **htelo** or **htelo-fl** in 100 mM NaCl, 10 mM Tris·HCl pH 7.4 was made up. This was heated to 90 °C for 10 min, allowed to cool slowly to room temperature, and stored at 4 °C. Where a potassium-containing solution was required, 100 mM KCl was used instead of NaCl.

**UV Melting Studies.** The absorbance at 295 nm ( $A_{295}$ )<sup>24</sup> of 1  $\mu$ M **htelo** or **htelo-fl** in 100 mM NaCl, 10 mM Tris·HCl pH 7.4 vs a 100 mM NaCl, 10 mM Tris·HCl pH 7.4 reference was monitored while the temperature was ramped between 10 and 90 °C at 0.5 °C min<sup>-1</sup>.

The samples were covered with mineral oil to prevent evaporation, and dry nitrogen was passed through the sample chamber to prevent condensation. Additional UV melts of **htelo-fl** were performed at strand concentrations of 0.5 and 4  $\mu$ M.

Linear baselines were fit to the high- and low-temperature regions of the resulting curve. The fraction folded, and hence equilibrium constant, at each temperature was determined from the position of the curve between these baselines. The melting temperature was determined from a van't Hoff analysis of those points for which the fraction folded was between 15% and 85%.<sup>21</sup> This method assumes a two-state system with linear baselines. Further it makes the assumption that there is no change in heat capacity due to (un)folding and that  $\Delta H$  and  $\Delta S$  are independent of temperature.

**Circular Dichroism (CD) Spectroscopy.** CD spectra of 1  $\mu$ M **htelo** or **htelo-fl** in 100 mM NaCl, 10 mM Tris·HCl pH 7.4 were taken at 20 °C between 220 and 320 nm. Ten scans were averaged for each sample. A background CD spectrum of 100 mM NaCl, 10 mM Tris·HCl pH 7.4 was subtracted.

**Fluorescence Spectroscopy.** Fluorescence spectra were taken of 120 nM **htelo-fl** in 100 mM NaCl, 10 mM Tris·HCl pH 7.4, and then 3 h after the addition of 5  $\mu$ M of the appropriate PNA. The temperature of the sample was set at 20 °C throughout.

Spectra were collected between 530 and 750 nm while exciting at 515 nm, and corrected for background fluorescence and instrument response. The contribution from direct excitation of Cy5 was neglected. The intensities of the individual fluorophores were calculated by integrating the fluorescence spectra from 565 to 620 nm for the donor (TMR) and 645 to 700 nm for the acceptor (Cy5). Fifteen percent of the donor integral was subtracted from that of the acceptor to correct for crosstalk. This value was determined from a similar analysis performed on an oligonucleotide conjugated to only TMR (data not shown). The proximity ratio,  $P$ , was calculated as

$$P = \frac{I_A}{I_A + I_D} \quad (1)$$

where  $I_D$  and  $I_A$  are the intensities of the donor and acceptor, respectively.

The proximity ratio is a useful measure of the extent of energy transfer between two fluorophores and is essentially the fraction of the total observed fluorescence emitted by the acceptor. Unlike the FRET efficiency,  $P$  cannot be used to calculate the distance between the fluorophores. However it has the advantage of being simpler to calculate and is useful if qualitative or relative distance information is all that is required.

**Fluorescence Kinetics.** For each kinetics run solution containing **htelo-fl** or **cPNA**, 100 mM NaCl and 10 mM Tris·HCl pH 7.4 were mixed at time  $t = 0$ . The final concentration of **cPNA** was 0.1, 1, 2.5, or 5  $\mu$ M, and that of **htelo-fl** was 100 nM, except that 10 nM **htelo-fl** was used for 0.1  $\mu$ M **cPNA**. This was to keep the concentration of **htelo-fl** an order of magnitude less than that of **cPNA**, so that the concentration of the latter could be assumed to be constant throughout the run.

Kinetics runs were performed at 10, 20, 37, and 50 °C. Samples were allowed to equilibrate before mixing, and dry air was passed through the sample chamber at 10 °C to prevent condensation.

The sample was excited at 515 nm, and the emission at 660 nm was measured every 5 s for 3 h. This wavelength, rather than 580 nm, was chosen in order to improve the sensitivity of the measurements, as it was found that the emission of Cy5 (660 nm) changed to a greater extent than that of TMR (580 nm). This may be due to partial quenching of TMR in the open conformation due to the close proximity of a guanine tract.<sup>25</sup>

(17) Egholm, M.; Buchardt, O.; Christensen, L.; Behrens, C.; Freier, S. M.; Driver, D. A.; Berg, R. H.; Kim, S. K.; Norden, B.; Nielsen, P. E. *Nature* **1993**, *365*, 566–568.

(18) Datta, B.; Armitage, B. A. *J. Am. Chem. Soc.* **2001**, *123*, 9612–9619.

(19) Moyzis, R. K.; Buckingham, J. M.; Cram, L. S.; Dani, M.; Deaven, L. L.; Jones, M. D.; Meyne, J.; Ratliff, R. L.; Wu, J.-R. *Proc. Natl. Acad. Sci. U.S.A.* **1988**, *85*, 6622–6626.

(20) Balagurumoorthy, P.; Brahmachari, S. K. *J. Biol. Chem.* **1994**, *269*, 21858–21869.

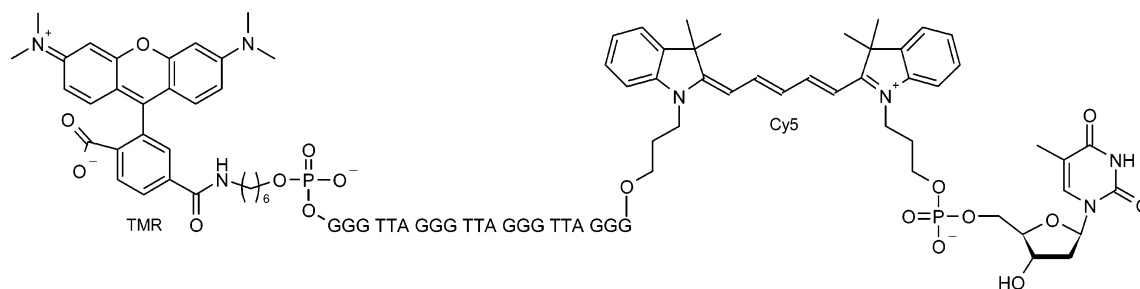
(21) Puglisi, J. D.; Tinoco, I., Jr. *Methods Enzymol.* **1989**, *180*, 304–325.

(22) From a table obtained from MWG Biotech.

(23) Values obtained from Applied Biosystems' PNA Quantification Calculator: <http://www.appliedbiosystems.com/support/concentration.cfm>, link at bottom of page.

(24) Mergny, J.-L.; Phan, A.-T.; Lacroix, L. *FEBS Lett.* **1998**, *435*, 74–78.

(25) Edman, L.; Mets, Ü.; Rigler, R. *Proc. Natl. Acad. Sci. U.S.A.* **1996**, *93*, 6710–6715.

Chart 3. Structure of **htelo-fl**

The portion of the kinetics trace over which a change in fluorescence intensity,  $F$ , was observed was fit to the double exponential decay

$$F = A_1 e^{-t/\tau_1} + A_2 e^{-t/\tau_2} + C \quad (2)$$

using the Solver module of Microsoft Excel, where  $t$  is the time after initiating measurements.  $\tau_1$  and  $\tau_2$  are the time constants of the decay and  $A_1$  and  $A_2$  their respective amplitudes.  $C$  is the fluorescence intensity at  $t = \infty$ .

The mean time constant,  $\langle \tau \rangle$ , was calculated as

$$\langle \tau \rangle = \frac{A_1 \tau_1 + A_2 \tau_2}{A_1 + A_2} \quad (3)$$

A double-exponential fit was chosen, as it consistently gave a much better fit to the data than a single-exponential decay, as judged by the residuals.

## Results

The focus of this study was to use FRET to monitor the unfolding of a quadruplex in the presence of a PNA oligomer complementary to the quadruplex-forming sequence. The sequence chosen was the minimal 21-mer human telomeric repeat sequence (**htelo**) capable of forming an intramolecular quadruplex. The fluorophores tetramethylrhodamine (TMR) and Cy5 were attached to the 5' and 3' termini, respectively, as shown in Chart 3, to give the dual-labeled oligonucleotide **htelo-fl**.

**CD Spectroscopy.** CD spectra of **htelo-fl** and **htelo** in 100 mM NaCl and 10 mM Tris·HCl pH 7.4 were taken in order to prove that under these buffer conditions the oligonucleotides were folded into quadruplexes. The results of this are shown in Figure 1. The peaks at 295 nm and troughs at 265 nm are consistent with the formation of antiparallel quadruplexes<sup>26</sup> for both **htelo** and **htelo-fl**. The presence of the fluorophores at the termini of the quadruplex alters the CD spectrum, as has been seen for a quadruplex labeled with fluorescein and TMR.<sup>14</sup> The change seen here is less extreme than that seen for this analogous dual-labeled oligonucleotide.<sup>14</sup>

**UV Melting of Quadruplexes.** UV melting curves of **htelo** and **htelo-fl** in 100 mM NaCl and 10 mM Tris·HCl pH 7.4 are shown in Figure 2. The melting temperature ( $T_m$ ) of **htelo-fl** ( $47 \pm 3$  °C) was lower than the value obtained for an **htelo** ( $58 \pm 3$  °C), indicating that the addition of the fluorophores destabilizes the structure. This reduction in melting temperature is comparable to that seen for an analogous fluorescein/TMR-labeled oligonucleotide.<sup>14</sup>

The UV melting temperatures for **htelo-fl** at 0.5, 1, and 4  $\mu$ M were found to be  $46 \pm 2$ ,  $47 \pm 3$ , and  $48 \pm 2$  °C, respectively. These melting temperatures are the same within

error, indicating that the transition observed is due to an intramolecular quadruplex.

**Fluorescence Spectroscopy.** Fluorescence spectra of **htelo-fl** were taken in the presence of complementary and noncomplementary 13-mer PNA oligomers (**cPNA** and **nPNA**, respectively). Spectra of **htelo-fl** in 100 mM NaCl and 10 mM Tris·HCl pH 7.4, alone and after additions of **nPNA** and **cPNA**, are shown in Figure 3. Their proximity ratios,  $P$ , were calculated to be  $0.78 \pm 0.01$ ,  $0.76 \pm 0.01$ , and  $0.39 \pm 0.01$ , respectively. This shows that addition of **nPNA** has little effect on the

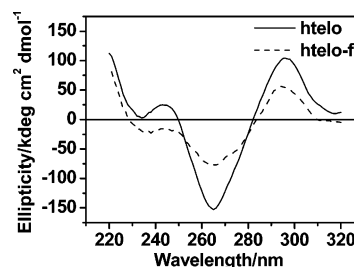


Figure 1. CD spectra of 1  $\mu$ M **htelo** and **htelo-fl** in 100 mM NaCl, 10 mM Tris·HCl pH 7.4. The traces are the smoothed averages of 10 scans.

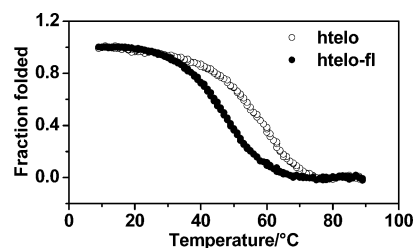


Figure 2. UV melting curves of 1  $\mu$ M **htelo** or **htelo-fl** in 100 mM NaCl, 10 mM Tris·HCl pH 7.4. The fraction folded was calculated from the original data assuming a two-state system with linear high- and low-temperature baselines.

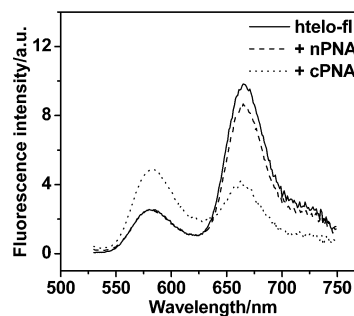
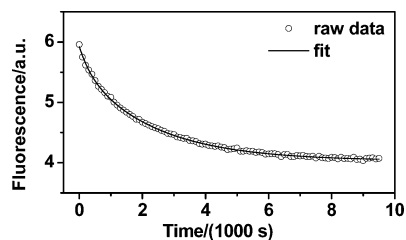


Figure 3. Fluorescence spectra of **htelo-fl** alone in 100 mM NaCl, 10 mM Tris·HCl pH 7.4 and after additions of **nPNA** and **cPNA**. Spectra were taken 3 h after each addition of PNA. The excitation wavelength was 515 nm, and spectra were recorded at 20 °C. The traces have been corrected for background fluorescence, instrument response, and changes in the concentration of **htelo-fl** caused by the addition of the PNA-containing solutions.



**Figure 4.** Example of a fluorescence intensity decay curve (exciting at 515 nm and collecting at 660 nm) after mixing **htelo-fl** (100 nM) with **cPNA** (1  $\mu$ M) in 100 mM NaCl, 10 mM Tris-HCl pH 7.4 at 20 °C. A double-exponential fit is superimposed on the data.

**Table 1.** Effects of **cPNA** Concentration ( $C$ ) and Temperature ( $T$ ) on the Mean Time Constant ( $\langle\tau\rangle$ ) and Rate Constant ( $k$ ) of the Opening of the **htelo-fl** Quadruplex

$C/\mu\text{M}$	$T/^\circ\text{C}$	$\langle\tau\rangle/\text{s}^a$	$k/10^{-5}\text{ s}^{-1}\text{ }^b$
1.0	20	1894 $\pm$ 61	53 $\pm$ 2
2.5	20	1918 $\pm$ 85	52 $\pm$ 3
5.0	20	1887 $\pm$ 93	53 $\pm$ 3
1.0	10	9871 $\pm$ 3438	11 $\pm$ 4
1.0	37	167 $\pm$ 18	600 $\pm$ 80
1.0	50	64 $\pm$ 9	1600 $\pm$ 300

<sup>a</sup> The values are the mean  $\pm$  standard deviation of three independent measurements. <sup>b</sup> Assumes hybridization is first-order in DNA and zero-order in PNA at all temperatures.

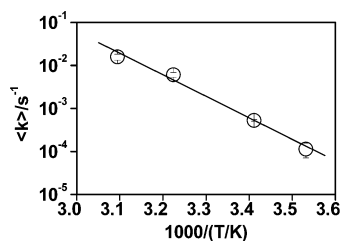


**Figure 5.** Arrhenius plot for the unfolding of the **htelo-fl** quadruplex in the presence of 1  $\mu$ M **cPNA**.

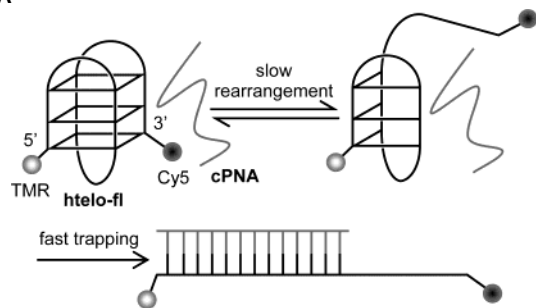
fluorescence properties of **htelo-fl**, while **cPNA** causes a large drop in proximity ratio. This is consistent with the opening of **htelo-fl** in the presence of **cPNA** due to the formation of a PNA:DNA duplex.

**Fluorescence Kinetics.** Solutions containing **htelo-fl** and **cPNA** were mixed at time  $t = 0$ , and the decay of the fluorescence of Cy5 was monitored. The resulting trace was fit to a double-exponential curve, and the inverse of the weighted mean of the measured time constants was taken as the rate constant of the unfolding reaction. The effects of **cPNA** concentration and temperature were examined.

An example of the data obtained in this study is shown in Figure 4. Studies carried out at 20 °C showed that the rate of decrease of Cy5 fluorescence is independent of **cPNA** concentration over the range 1–5  $\mu$ M (Table 1).<sup>27</sup> The activation energy of the unfolding of **htelo-fl** was derived from the Arrhenius plot (Table 1, Figure 5) to be  $98 \pm 8\text{ kJ mol}^{-1}$ , assuming that the mechanism is the same at all temperatures studied. The validity of this assumption is supported by the linearity of the graph, which would be unexpected if there was a change in rate-determining step.

Kinetics runs performed in the presence of 100 mM KCl rather than NaCl gave average time constants of about 40 h at

**Scheme 1.** Possible Mechanism for the Unfolding of **htelo-fl** with **cPNA**



20 °C and 4 h at 37 °C (data not shown), consistent with the formation of a significantly more stable quadruplex under these conditions as previously observed.<sup>20</sup> However, these time scales are too slow to obtain accurate kinetics data with our equipment.

## Discussion

**Steady-State Measurements.** Steady-state measurements were taken in order to confirm that the fluorescently labeled **htelo-fl** folds into a quadruplex as predicted under the experimental conditions employed. CD spectra of **htelo** and **htelo-fl** verified that both folded into antiparallel quadruplexes. UV melting experiments indicated that the melting temperature of **htelo-fl** was comparable to that of a fluorescein/TMR-labeled 21-mer DNA of the same sequence.<sup>14</sup> This indicates that both sets of fluorophores destabilize the quadruplex to a similar extent. The melting temperature was found to be independent of the concentration of **htelo-fl**, indicating that the quadruplex formed is intramolecular. The formation of an antiparallel intramolecular quadruplex is consistent with the NMR structure of the quadruplex formed by d[A(GGGTTA)<sub>3</sub>GGG] in the presence of 100 mM Na<sup>+</sup>.<sup>28,29</sup>

The addition of a noncomplementary PNA oligomer (**nPNA**) was shown to have little effect on the fluorescence spectrum of **htelo-fl**, while addition of complementary PNA (**cPNA**) greatly reduced the Cy5 fluorescence and thus the proximity ratio,  $P$ . This suggests that the interaction of **htelo-fl** with **cPNA** is due to its sequence complementarity rather than a nonspecific interaction with PNA.

**Kinetics Measurements.** The first-order kinetics observed here suggest a rearrangement of the quadruplex prior to trapping by **cPNA** in the overall unfolding process (Scheme 1). However, the structural details of this rearrangement cannot be determined from these results alone, and the intermediate shown in Scheme 1 is one of many possibilities. For example it is possible that **htelo-fl** must unfold completely in order to allow **cPNA** to hybridize.

From the unfolding rate and the equilibrium constant it is possible to estimate the rate of folding from

$$K_{\text{eq}} = \frac{k_f}{k_u} \quad (4)$$

where  $K_{\text{eq}}$  is the equilibrium constant and  $k_f$  and  $k_u$  are the folding and unfolding rate constants, respectively. The equilibrium constants for the folding of **htelo-fl** in 100 mM NaCl and 10 mM Tris-HCl pH 7.4 at 37 and 50 °C were determined from

(27) The unfolding kinetics were 20% slower at 100 nM **cPNA**, consistent with a transition to second-order kinetics at lower **cPNA** concentration.

(28) Wang, Y.; Patel, D. J. *Structure* **1993**, *1*, 263–282.

(29) Protein Data Bank 143D.

UV melting curves to be  $4 \pm 1$  and  $0.7 \pm 0.1$ , respectively. The equilibrium constants at 10 and 20 °C were too large to be determined by this technique. This estimates the closing rates at 37 and 50 °C to be  $(2.4 \pm 0.8) \times 10^{-2}$  and  $(1.1 \pm 0.3) \times 10^{-2} \text{ s}^{-1}$ , respectively, assuming the rate-determining step for unfolding is unaffected by the presence of **cPNA**. The closing rate at 37 °C is an order of magnitude faster than the folding rate reported for the quadruplex formed by  $d[(T_4G_4)_4]$  in 50 mM  $\text{Na}^+$  at 37 °C ( $1.7 \times 10^{-3} \text{ s}^{-1}$ ).<sup>30</sup> This difference may be caused by the presence of fluorophores in **htelo-fl**, which have been shown by UV melting to alter the thermodynamics of the quadruplex. Furthermore, the quadruplex formed by an oligonucleotide closely related to  $d[(T_4G_4)_4]$  has been shown to contain four tetrads,<sup>31</sup> while that formed by **htelo-fl** contains only three.

That the rearrangement of the quadruplex appears to be slower than the subsequent hybridization event is consistent with observations reported in a study of the opening of the quadruplex formed by  $d[(T_4G_4)_4]$  using a complementary DNA strand.<sup>30</sup> However, it differs from PNA hybridization to unstructured DNA<sup>32,33</sup> and DNA hairpins,<sup>33</sup> where PNA invasion was found to be first-order with respect to both components, making it second-order overall. The difference between the order of the hybridization of PNA to hairpins and quadruplexes may be explained by a simple preequilibrium model: the folded structure is in equilibrium with an intermediate, which then hybridizes to the complementary PNA strand (Scheme 1). If PNA hybridization is the rate-determining step, the reaction will be second-order. If, however, the formation of the intermediate is rate determining, first-order kinetics will be observed.

In the case of the hairpin the opening rate at 20 °C is on the order  $10^2$ – $10^3 \text{ s}^{-1}$ ,<sup>34,35</sup> while the results presented here suggest an opening rate for the quadruplex of  $5 \times 10^{-4} \text{ s}^{-1}$ . The hybridization rate of an unstructured 8-mer DNA strand to PNA serves as a useful reference. This was found to be  $2 \times 10^3 \text{ M}^{-1} \text{ s}^{-1}$ ,<sup>33</sup> giving a pseudo-first-order rate constant of  $2 \times 10^{-3} \text{ s}^{-1}$

for 1  $\mu\text{M}$  PNA. This is faster than the unfolding of the quadruplex but slower than that of the hairpin, providing a possible explanation for the observed reaction orders for hybridizations of the quadruplex and hairpin to PNA.

The activation energy measured here is comparable in magnitude to those measured for the dissociation of the intermolecular quadruplexes formed by  $d(\text{TATG}_4\text{ATA})_4$  and  $d(\text{CGCG}_4\text{CG})_4$ , determined by CD spectroscopy to be 200 and 150  $\text{kJ mol}^{-1}$ , respectively.<sup>36</sup> The differences are possibly due to additional stability in these intermolecular quadruplexes arising from the additional tetrad, interactions with adenines in the former, and  $\text{C}\cdot\text{C}^+$  base pairing in the latter. Other potential factors include the loops in **htelo-fl**, which are not present in the intermolecular quadruplexes, and that these intermolecular quadruplexes are parallel,<sup>36,37</sup> while the structure formed by **htelo-fl** in sodium is antiparallel. It is also possible that the destabilization of the **htelo-fl** quadruplex due to the presence of the fluorophores lowers the activation energy.

## Conclusions

We have investigated the opening of the intramolecular quadruplex formed by the human telomeric repeat. A complementary 13-mer PNA was employed to trap the structure as it unfolded, and the hybridization was monitored using FRET between a pair of fluorophores conjugated to the termini of the oligonucleotide. The use of FRET allowed real-time monitoring of the opening process at significantly lower concentrations than would have been possible with UV absorbance or CD.

It was observed that the opening of the quadruplex was independent of PNA concentration, suggesting that the initial step is a rate-determining internal rearrangement of the quadruplex, followed by a fast hybridization step. An Arrhenius analysis of the system gave an activation energy of  $98 \pm 8 \text{ kJ mol}^{-1}$ , which is comparable in magnitude to values found for other quadruplexes.

**Acknowledgment.** We thank Gérald Gavory and Dr. Yamuna Krishnan-Ghosh for providing the PNA samples, and the BBSRC for funding.

JA029149W

(30) Raghuraman, M. K.; Cech, T. R. *Nucleic Acids Res.* **1990**, *18*, 4543–4552.

(31) Wang, Y.; Patel, D. J. *J. Mol. Biol.* **1995**, *251*, 76–94.

(32) Jensen, K. K.; Ørum, H.; Nielsen, P. E.; Nordén, B. *Biochemistry* **1997**, *36*, 5072–5077.

(33) Kushon, S. A.; Jordan, J. P.; Seifert, J. L.; Nielsen, H.; Nielsen, P. E.; Armitage, B. A. *J. Am. Chem. Soc.* **2001**, *123*, 10805–10813.

(34) Bonnet, G.; Krichevsky, O.; Libchaber, A. *Proc. Natl. Acad. Sci. U.S.A.* **1998**, *95*, 8602–8606.

(35) Wallace, M. I.; Ying, L.; Balasubramanian, S.; Klenerman, D. *Proc. Natl. Acad. Sci. U.S.A.* **2001**, *98*, 5584–5589.

(36) Hardin, C. C.; Corregan, M.; Brown, B. A., II; Frederick, L. N. *Biochemistry* **1993**, *32*, 5870–5880.

(37) Hardin, C. C.; Watson, T.; Corregan, M.; Bailey, C. *Biochemistry* **1992**, *31*, 833–841.